SPANDIDOS PUBLICATIONS

ONCOLOGY LETTERS 16: 2725-2731, 2018

Performance of Gd-EOB-DTPA-enhanced MRI for the diagnosis of LI-RADS 4 category hepatocellular carcinoma nodules with different diameters

QI TANG[1] and CONG MA[2]

Departments of [1]Surgery and [2]Radiology, The Second XiangYa Hospital of Central South University, Changsha, Hunan 410011, P.R. China

Received August 24, 2017; Accepted February 16, 2018

DOI: 10.3892/ol.2018.8884

Abstract. In 2011, the American College of Radiology released a standardized reporting and data collection system, named Liver Imaging Reporting and Data System (LI-RADS), to improve the consistency of diagnostic imaging examinations of hepatocellular carcinoma (HCC). When the LI-RADS guideline was updated in 2014, hepatobiliary contrast agents, including gadoxetate acid (Gd-EOB-DTPA), were incorporated into the system. However, the diagnostic performance of Gd-EOB-DTPA-enhanced magnetic resonance imaging (MRI) for nodules of different diameters has not been addressed. In the present study, a total of 263 LI-RADS 4 category hepatic nodules were examined blindly and independently by two radiologists. All nodules were divided into two datasets: Set 1 (n=86) that included nodules with iso/hypo-intensity in the arterial phase (HCC, n=42; non-HCC, n=44) and set 2 (n=177) that included nodules with hyper-intensity in the arterial phase (HCC, n=131; non-HCC, n=46). The diagnostic performance of Gd-EOB-DTPA-enhanced MRI for evaluation of nodules with different diameters was evaluated. The present study revealed that the diagnostic performance of Gd-EOB-enhanced MRI of larger nodules (>2 cm) was higher compared with (<2 cm) smaller nodules. The FPR of large nodules (>2 cm) with a hypervascular pattern was lower compared with smaller nodules (<2 cm) with hypovascular pattern. In conclusion, Gd-EOB-enhanced MRI is useful for the diagnosis of HCC where hypervascular LI-RADS 4 nodules are >2 cm in diameter. However, Gd-EOB-enhanced MRI may be of limited use for the assessment of nodules that <20 mm due to low diagnostic performance and high FPR.

Correspondence to: Dr Cong Ma, Department of Radiology, The Second Xiangya Hospital of Central South University, 139 Middle Renmin Road, Changsha, Hunan 410011, P.R. China
E-mail: mcismc@126.com

Abbreviations: MR, magnetic resonance; LI-RADS, Liver Imaging Reporting and Data System; HCC, hepatocellular carcinoma; PPV, positive predictive value; NPV, negative predictive value; FPR, false positive rate; CT, computed tomography; Gd-EOB-DTPA, gadoxetate acid; HBP, hepatobiliary phase; RFA, radiofrequency ablation; ICC, intraclass correlation coefficient; HGDN, high-grade dysplastic nodules; LGDN, low-grade dysplastic nodules; cHCC-CCCs, combined cholangiocarcinoma and hepatocellular carcinoma; TP, true positive; FP, false positive; FN, false negative; TN, true negative

Key words: gadoxetic acid, diagnostic performance, magnetic resonance imaging, hepatocellular carcinoma

Introduction

Hepatocellular carcinoma (HCC) is a global health problem, and it is a major cause of mortality in cirrhotic patients (1-3). Patients with liver cirrhosis are strongly recommended to undergo routine liver imaging for surveillance of HCC (4). According to current guidelines, HCC can be diagnosed using typical imaging criteria, including hypervascularity in the hepatic arterial phase and washout in a later phase on dynamic contrast-enhanced computed tomography (CT) and/or magnetic resonance imaging (MRI) (5-8). To improve the consistency of imaging diagnosis of HCC, the American College of Radiology has released a standardized reporting and data collection system known as Liver Imaging Reporting and Data System (LI-RADS) in 2011 (9). When the guideline was updated in 2014, hepatobiliary contrast agents, including gadoxetate acid (Gd-EOB-DTPA) and gadobenate dimeglumine (Gd-BOPTA) were incorporated into the system (10). However, findings in the hepatobiliary phase (HBP) are ancillary features that can be applied to upgrade or downgrade categories using tie-breaking rules (11). This can be used up to LI-RADS 4 but not beyond (12).

Recently, Chen *et al* (13) reported that hypointensity in HBP may be a criterion that can improve the sensitivity of LI-RADS in HCC diagnosis where Gd-EOB-DTPA-enhanced MR with HBP imaging and a modified 2014 version of the LI-RADS were used. Although LI-RADS is essential for the diagnosis of HCC (14), the diagnostic performance of Gd-EOB-DTPA-enhanced MRI in nodules of different diameter has not been addressed. The definition of LI-RADS 4 category nodules is probably HCC. The most important factor when diagnosing a focal liver lesion is to differentiate between LI-RAD category 4 and 5 nodules, where LI-RADS

category 5 is definitely HCC and LI-RADS category 4 is probably HCC (15). Therefore, the present study aims to evaluate the diagnostic performance of Gd-EOB-DTPA dynamic contrast-enhanced MRI of LI-RADS 4 hepatic nodules of various diameters.

Materials and methods

Patient selection. This retrospective study was approved by the Institutional Review Board in accordance with the approved guidelines from the Second Xiangya Hospital of Central South University (Hunan, China) and was compliant with Health Insurance Portability and Accountability Act (HIPAA). Written informed consent was obtained from all patients.

A search of the Picture Archiving and Communication Systems (the Second Xiangya Hospital of Central South University) was performed between October 2012 and June 2016. A total of 778 patients with chronic liver cirrhosis who underwent Gd-EOB-DTPA-enhanced MRI for the detection of suspected liver lesions were enrolled. As one of the primary criteria of using LI-RADS is that the patients are of cirrhotic background, only patients with liver cirrhosis were included (16). The inclusion criteria were as follows: i) Patients have not received locoregional therapy, including transarterial chemoembolization or radiofrequency ablation (RFA), ii) nodule size was ≤30 mm, iii) and number of nodules was ≤5 on MRI. Each nodule was assigned to a LI-RADS category according to the 2017 version of LI-RADS: LI-RADS 1, definitely benign; LI-RADS 2, probably benign; LI-RADS 3, intermediate probability of HCC; LI-RADS 4, probably HCC, LI-RADS 5, definitely HCC, LI-RADS TIV, definitely tumor in vein and LI-RADS M, probably malignant, not specific for HCC (17). Only LI-RADS 4 nodules were included in the present study. After applying the inclusion criteria, the study population comprised 224 patients with 263 nodules. The study population consisted of 138 males and 86 females with an age range of 26-81 years and a mean age of 53.3±17.1 years.

MR imaging technique. MR imaging was performed using a clinical 3.0 Tesla superconducting MR system (MAGNETOM Skyra; Siemens Healthineers, Erlangen, Germany) with an 18-channel body matrix coil and an inbuilt 24-channel spine matrix coil. The comprehensive MRI protocol, including T1-weighted fat saturation gradient recalled echo sequence and T2-weighted half-Fourier acquisition single-shot turbo spin-echo sequence, were obtained prior to the administration of Gd-EOB-DTPA (Bayer Schering Pharma, Berlin, Germany). Dynamic contrast-enhanced MRI was performed using a combination of volume interpolated breath-hold examination (VIBE) with controlled aliasing in parallel imaging results in higher acceleration (CAIPIRINHA), view-sharing time-resolved imaging with interleaved stochastic trajectories (TWIST), Dixon fat suppression (CAIPIRINHA-Dixon-TWIST-VIBE and CDT-VIBE) in the unenhanced phase, arterial phase, portovenous phase (90 secs), transitional phase (180 secs) and HBP (20 min). In order to ensure that the same contrast-enhanced phase is attained in each patient, a MR automated injector pump was used to administer Gd-EOB-DTPA through an 18-gauge cubital intravenous access at a dose of 0.1 ml/kg body weight and an injection rate of 1 ml/sec. The MR parameters are listed in Table I.

Table I. Magnetic resonance sequence parameters.

Parameters	CDT-VIBE	T2 HASTE
TR/TE, msec	3.8/1.2	2,000/80
Subphases	5	1
Sequence type	TWIST-VIBE	HASTE
Voxel size, mm^3	1.3x1.3x3.0	1.3x1.3x3.0
FOV, mm	380	380
Slice number	72	72
Flip angle, degree	9	180
Respiratory control	Breath hold	Triggered
Fat suppression	Dixon	Spectral saturation
Temporal resolution, s	2.6	-
TWIST size of k-center, %	20	-
TWIST size of k-periphery, %	25	-
Breath-holding time, sec	20	10-15

FOV, field of view; HASTE, half-Fourier acquisition single-shot turbo spin-echo; TR, time of repletion; TE, time of echo; VIBE, volume-interpolated breath-hold examination.

Imaging analysis. A total of two radiologists with 20-years and 12-years liver imaging experience randomly and independently reviewed all images. Both radiologists were blinded to the LI-RADS category and the final diagnosis of each nodule. The major criteria of LI-RADS, including arterial phase enhancement patterns, nodule diameter, presence or absence of washout in the portal venous phase, presence or absence of capsule and threshold growth, were evaluated. Due to early liver parenchymal enhancement following the administration of Gd-EOB-DTPA, only portal venous phase hypo-intensity and not transitional phase hypo-intensity was considered as a washout appearance. Ancillary features that favored malignancy, including transitional phase hypo-intensity, mild-moderate T2 hyper-intensity, restricted diffusion, mosaic architecture, nodule-in-nodule architecture, corona enhancement and intralesional fat were also reviewed. The images were reviewed independently, and the diagnosis of each nodule was made in consensus between the two radiologists.

Statistical analysis. Statistical analysis was performed using software SPSS (version 20.0; IBM Corp., Armonk, NY, USA). A Cohen's kappa test was performed to evaluate the inter-reader agreement of LI-RADS major criteria, including arterial phase enhancement patterns, presence or absence of washout in the portal venous phase, presence or absence of capsule and HBP enhancement patterns. Intraclass correlation coefficient (ICC) was performed to evaluate the inter-reader agreement of nodules diameter measurement. Agreement was classified as poor (K, 0-0.40), fair to good (K, 0.40-0.75) or excellent (K, >0.75). According to the results by the two radiologists,

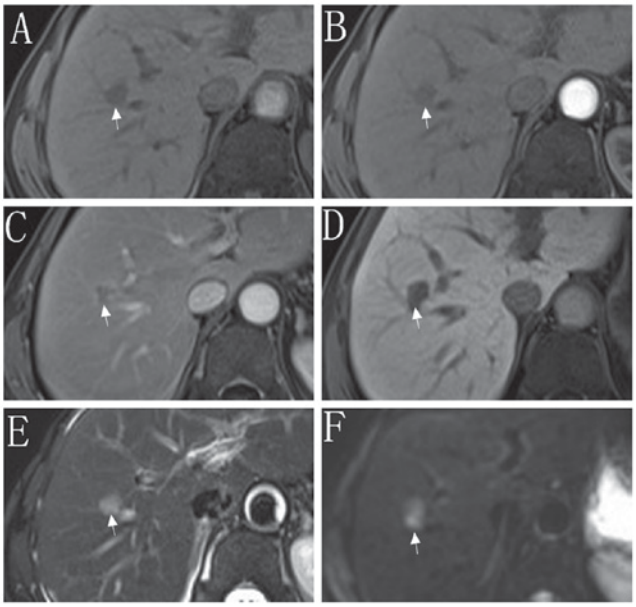

Figure 1. Gadoxetate acid-enhanced magnetic resonance images in a 50 year-old man with hepatitis B-induced liver cirrhosis. (A) Pre-contrast magnetic resonance images indicated a 16-mm nodule (arrow) in the right lobe of the liver. (B) The nodule was indicated to be hypo-intense in the hepatic arterial phase; (C) to have a washout appearance with the absence of a capsule in the portal venous phase; (D) hypo-intense in the hepatobiliary phase. The nodule was categorized according to Liver Imaging Reporting and Data System 4 with ancillary findings of (E) mild-moderate T2 hyper-intensity and (F) restricted diffusion.

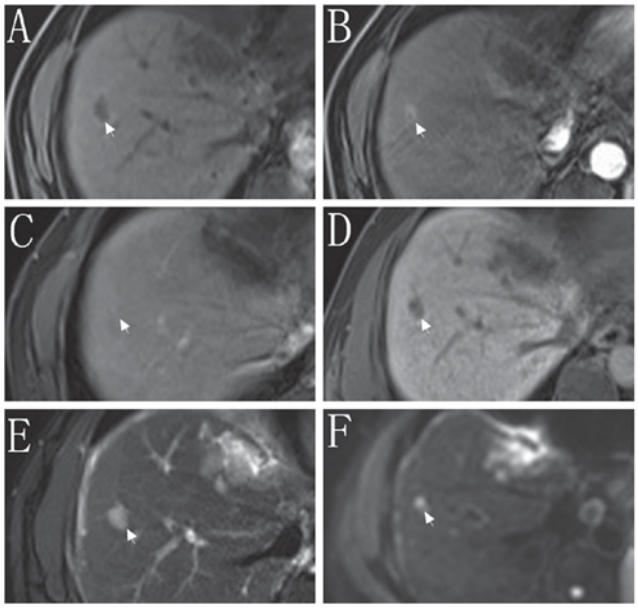

Figure 2. Gadoxetate acid-enhanced magnetic resonance images in a 43 year-old man with hepatocellular carcinoma recurrence following surgical resection. (A) Pre-contrast magnetic resonance images indicated a 12-mm nodule (arrow) in the right lobe of the liver. The nodule was indicated to be (B) hyper-intense in the hepatic arterial phase, (C) iso-intense and with the absence of capsule in the portal venous phase and (D) hypo-intense in the hepatobiliary phase. The nodule was categorized according to Liver Imaging Reporting and Data System 4 with ancillary findings of (E) mild-moderate T2 hyper-intensity and (F) restricted diffusion.

nodules diagnosed as probably or definitely HCC were positive results, and probably or definitely not HCC nodules were negative results. The sensitivity, specificity, positive predictive value (PPV) and negative predictive value (NPV) for the diagnosis of HCC nodules of different diameters using LI-RADS 4 were calculated and expressed with 95% confidence intervals (CI). The false positive rate (FPR) was also calculated.

Results

Patient characteristics. The study population consisted of 138 males and 86 females, with an age range of 26-81 years and a mean age of 53.3±17.1 years. Of the 263 nodules, the diameter of the 173 HCC nodules was 22.4±7.1 mm. The diameter of the 26 non-HCC malignant nodules was 16.6±6.5 mm, and the diameter of the remaining 64 benign nodules was 12.7±4.3 mm. The HCC nodules were significantly larger compared with the non-HCC malignant nodules ($P<0.05$) and benign nodules ($P<0.05$). The 2017 version of LI-RADS categorizes nodules primarily based on the arterial phase enhancement patterns (17). In accordance with LI-RADS, the data on 263 nodules were divided into two datasets: Set 1 (n=86) that contain nodules with iso/hypo-intensity at the arterial phase (HCC, n=42; non-HCC, n=44) and set 2 (n=177) that contain nodules with hyper-intensity at the arterial phase (HCC, n=131; non-HCC, n=46). The typical imaging appearance of sets 1 and 2 are indicated in Figs. 1 and 2, respectively. Of the 86 nodules in set 1, 37 nodules were <20 mm in diameter (set 1A), and 49 nodules were 20-30 mm in diameter (set 1B). Of the 177 nodules in set 2, 68 nodules were <10 mm in diameter (set 2A) and 73 nodules were 10-19 mm in diameter (set 2B). A further 36 nodules were 20-30 mm in diameter (set 2C). The detailed information is listed in Table II.

Inter-reader agreement between two reviewers. Cohen's Kappa test and the ICC indicated that inter-reader agreement of the LI-RADS major criteria and HBP imaging ranged from fair to good to excellent. Specifically, the measurements for nodule diameter exhibited excellent agreement between LI-RADS and HBP imaging with an ICC value of 0.951. Other characteristics, including HBP enhancement patterns, arterial phase enhancement patterns and presence or absence of washout, exhibited excellent inter-reader agreement with K values of 0.937, 0.814 and 0.762, respectively. Finally, the presence or absence of capsule exhibited fair to good agreement with a K value of 0.681.

Final diagnosis of the nodules. Each of the 263 nodules in 224 patients was conclusively diagnosed as HCC (173 nodules in 146 patients) or non-HCC (90 nodules in 78 patients). The 90 non-HCC nodules were further diagnosed as follows: High-grade dysplastic nodules (HGDN), 22 nodules in 22 patients; low-grade dysplastic nodules (LGDN), 16 nodules in 16 patients; regenerative nodules, 14 nodules in 13 patients; liver metastasis, 14 nodules in 9 patients; atypical hemangioma, 7 nodules in 6 patients; atypical intrahepatic cholangiocarcinoma, 10 nodules in 7 patients; combined cholangiocarcinoma/HCC (cHCC-CCCs), 2 nodules in 2 patients and hepatocellular adenoma, 5 nodules in 3 patients. The final diagnosis of the nodules was made based on histologic proof (surgical resection, n=23; biopsy, n=161), follow-up >12 months (n=9) or tumor recurrence/metastasis following treatment (n=70). Of the

Table II. Clinical characteristics of 263 nodules.

Variables	Total (n=263)
Diameter of nodules, mm	-
HCC	22.4±7.1
Non-HCC malignancy	16.6±6.5
Benign	12.7±4.3
Number of nodules, HCC/non-HCC	-
Set 1	42/44
Set 1A	15/22
Set 1B	27/22
Set 2	131/46
Set 2A	50/18
Set 2B	53/20
Set 2C	28/8

Set 1A, hypovascular nodules with a diameter of <20 mm; Set 1B, hypovascular nodules with a diameter of 20-30 mm; Set 2A, hypervascular nodules with a diameter of <10 mm; Set 2B, hypervascular nodules with a diameter of 10-19 mm; Set 2C, hypervascular nodules with a diameter of 20-30 mm. HCC, hepatocellular carcinoma.

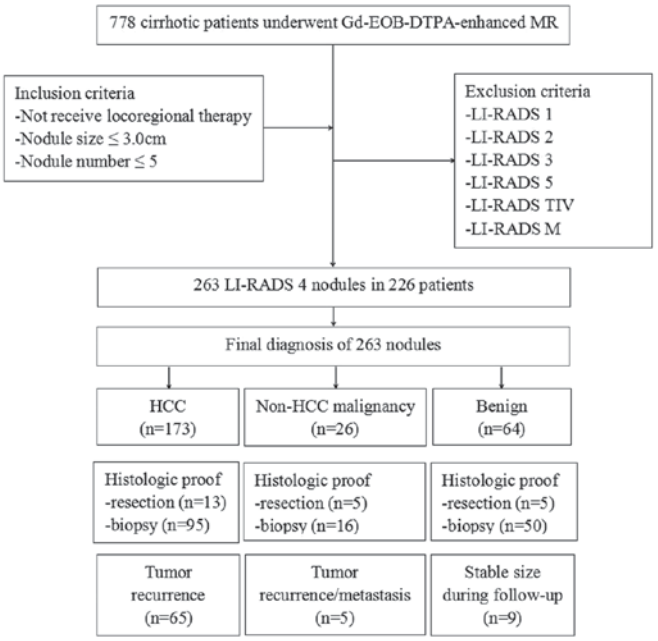

Figure 3. Diagram illustrating patient selection in the present study. Gd-EOB-DTPA, gadoxetate acid; HCC, hepatocellular carcinoma; MR, magnetic resonance; LI-RADS, liver imaging reporting and data system; TIV, tumor in vein.

Table III. Results of nodules according to the final diagnosis.

Groups	TP	FP	FN	TN
Set 1A, n	9	14	6	8
Set 1B, n	20	9	7	13
Set 2A, n	31	9	19	9
Set 2B, n	37	7	16	13
Set 2C, n	26	1	2	7
Entire population, n	123	40	50	50

Set 1A, hypovascular nodule with a diameter <20 mm; Set 1B, hypovascular nodule with a diameter of 20-30 mm; Set 2A is hypervascular nodule with a diameter <10 mm; Set 2B, hypervascular nodule with a diameter of 10-19 mm; Set 2C, hypervascular nodule with a diameter of 20-30 mm; TP, true positive; FP, false positive; FN, false negative; TN, true negative.

173 HCC nodules, 108 nodules were confirmed by histologic proof (surgical resection, n=13; biopsy, n=95), while 65 nodules appeared during tumor recurrence following treatment. Of the 90 non-HCC nodules, 76 nodules were confirmed by histologic proof (surgical resection, n=10; biopsy, n=66), 9 nodules were of a stable size during follow-up, and 5 nodules appeared during tumor recurrence/metastasis following treatment. A flowchart of the study population is shown in Fig. 3.

Diagnostic performance in each subgroup. Based on the final diagnosis of all 263 nodules, the diagnosis of 123 nodules were true positive (TP), 40 nodules were false positive (FP) and 50 nodules were false negative (FN) results. The remaining 50 nodules were true negative (TN) results. The detailed results are listed in Table III.

For the diagnosis of HCC, the sensitivity, specificity, PPV and NPV of Gd-EOB-DTPA-enhanced MR for the entire study population were 71.1% (95% CI, 63.6-77.6), 55.6% (95% CI, 44.7-65.9), 75.5% (95% CI, 68.0-81.7) and 50% (95% CI, 39.9-60.1), respectively. For set 1B, the sensitivity, specificity, PPV and NPV were 74.1% (20/27), 59.1% (13/22), 69.0% (20/29) and 65.0% (13/20), respectively. For set 2C, the sensitivity, specificity, PPV and NPV were 92.8% (26/28), 87.5% (7/8), 96.3% (26/27) and 77.8% (7/9), respectively. When the diagnostic performance of set 1 and set 2 was compared, set 2 exhibited relatively higher sensitivity, specificity, PPV, and NPV compared with set 1 in each subgroup. The diagnostic performance of Gd-EOB-DTPA-enhanced MR of nodules with different diameters in set 1 and set 2 are summarized in Table IV. For FPR, the nodules in set 2C exhibited the lowest FPR within all subgroups (12.5%, 1/8). A MRI image of a false positive result is indicated in Fig. 4.

Discussion

Small hepatic lesions can be more challenging to characterize. Several studies have shown that small intrahepatic cholangiocarcinoma, hemangioma, and metastases may mimic the enhancement characteristics of HCC (18-20). Unlike the LI-RADS 5 category, which has a low cut-off value for diameter (1 cm), LI-RADS 4 applies the same high probability of HCC for lesions of varying sizes, including those with a diameter of <1 cm. It is unclear if the malignancy rate and predictive ability of LI-RADS 4 should apply to small (<2 cm) and large lesions (>2 cm) or whether specific features such as a combination of HBP hypointensity and arterial phase hyper-enhancement may provide a means for improving specificity.

The results indicated that, Gd-EOB-DTPA-enhanced MR provides higher diagnostic performance for nodules of a larger

Table IV. Diagnostic performance of Gd-EOB-DTPA-enhanced MR for LI-RADS 4 nodules.

	Set 1, % (95% CI)	Set 1B, %	Set 2A, %	Set 2B, %	Set 2C, %
Sensitivity	60.0 (32.9-82.5)	74.1 (53.4-88.1)	62.0 (47.2-75.0)	69.8 (55.5-81.3)	92.8 (75.0-98.7)
Specificity	36.4 (18.0-59.1)	59.1 (36.7-78.5)	50.0 (26.8-73.2)	65.0 (40.9-83.7)	87.5 (46.7-99.3)
PPV	39.1 (20.5-61.2)	69.0 (49.0-84.0)	77.5 (66.1-88.6)	84.1 (69.3-92.8)	96.3 (79.1-99.8)
NPV	57.1 (29.6-81.2)	65.0 (40.9-83.7)	32.1 (16.6-52.4)	44.8 (26.9-64.0)	77.8 (40.2-96.0)

Set 1A, hypovascular nodule with a diameter of <20 mm; Set 1B, hypovascular nodule with a diameter of 20-30 mm; Set 2A, hypervascular nodule with a diameter of <10 mm; Set 2B, hypervascular nodule with a diameter of 10-19 mm; Set 2C, hypervascular nodule with a diameter of 20-30 mm. CI, confidence interval; PPV, positive predict value; NPV, negative predict value.

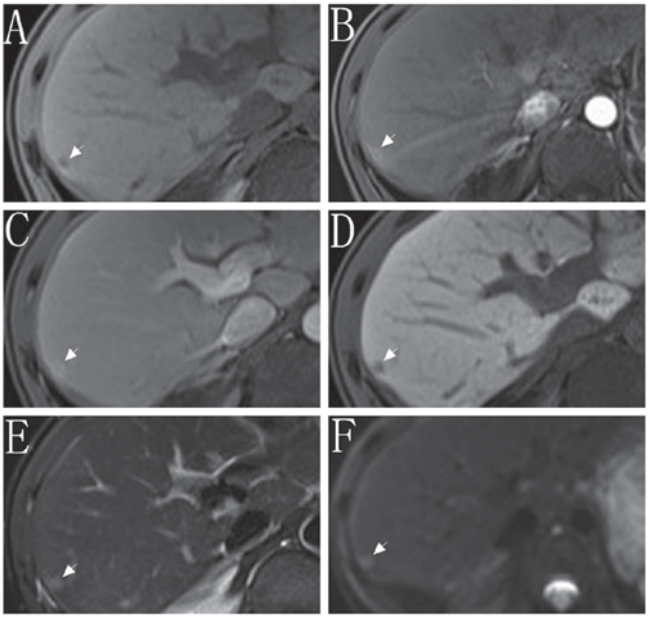

Figure 4. False positive result in a 40 year-old man with chronic hepatitis B. The final diagnosis of this nodule was intrahepatic cholangiocarcinoma. (A) Pre-contrast magnetic resonance images indicated a 8-mm nodule (arrow) in the right lobe of the liver. (B) The nodule was indicated to be hyper-intense in the hepatic arterial phase, (C) hyper-intense with the absence of capsule in the portal venous phase, and (D) hypo-intense in the hepatobiliary phase. The nodule was categorized according to Liver Imaging Reporting and Data System 4 with ancillary findings of mild-moderate (E) T2 hyper-intensity and (F) restricted diffusion.

size (>2 cm) than a smaller size (<2 cm). In a previous study on the diagnosis of HCC, Chen *et al* (13) showed that HBP hypointensity was a major criterion of LI-RADS that could provide sensitivity, specificity, PPV, and NPV of 95, 96, 99 and 87%, respectively. The results in the present study differ from the findings of Chen *et al* (13). In the present study, the diagnostic performance is as high as the values reported in Chen *et al* (13) but only for nodules with a diameter of 20-30 mm with sensitivity, specificity, PPV, and NPV of 92.8, 87.5, 96.3 and 77.8%, respectively. Differences in the inclusion criteria used in the two studies may account for this discrepancy. The study by Chen *et al* (13) included LI-RADS 1-5 category nodules, while only the LI-RADS 4 category nodules are included in the present study, which may affect sensitivity and specificity calculation. Notably, a previous study conducted by Darnell *et al* (21) revealed that in cirrhosis patients for the diagnosis of HCC, the MRI findings of LI-RADS 4 and 5 category nodules have a sensitivity of 65.4% and specificity of 98.2%. However, the sensitivity value in the present study is higher than the value reported by Darnell *et al* (21) (92.8% vs. 65.4%). Conversely, the specificity is lower in the present study (87.5% vs. 98.2%), which may be due to the different contrast agents used in the two studies (Gd-EOB-DTPA vs. gadodiamide.

We analyzed FPR to determine which types of nodules were more easily misdiagnosed as HCC. It was detected that nodules with a diameter of 20-30 mm with a hypervascular pattern exhibited the lowest FPR (12.5%, 1/8). However for nodules with a diameter of <10 mm, the FPR was as high as 63.6% (14/22). Although it has been reported that Gd-EOB-DTPA-enhanced MRI is able to detect hypovascular lesions (22-24), nodules with arterial phase enhancement remains a primary element for HCC. One of the main false positive results for hypovascular nodules is dysplastic nodule. A high HGDN, in its initial phase of carcinogenesis, can present as hypo-intensity in the arterial phase with gradual enhancement in portal venous phase due to the presence of portal perfusion (25). With the increase of intra-nodular arterial vascularity, the enhancement pattern for HGDN tends to be hypervascularity (26). This is the main reason that HGDN mimicked HCC in the present study. The other main false positive result is intrahepatic cholangiocarcinoma. It has been reported that the most frequent enhancement pattern for intrahepatic cholangiocarcinoma in normal liver is a thin peripheral rim with internal heterogeneous enhancement during the dynamic phase (27). However, intrahepatic cholangiocarcinoma in patients with or without liver cirrhosis may differ in enhancement pattern (28). In patients with liver cirrhosis, intrahepatic cholangiocarcinoma is often characterized as a stable enhancement pattern, particularly for nodules <20 mm in diameter (29,30). In the present study, the majority of intrahepatic cholangiocarcinoma cases present a similar enhancement pattern to the previous studies (31). Hemangioma is another notable false positive result. The typical enhancement pattern for hemangioma is delayed phase enhancement on extracellular contrast agent based-enhanced imaging (32). However, previous studies report that a 'pseudo washout' sign can be observed in hemangioma during the transitional phase using Gd-EOB-DTPA as the contrast agent, probably owing to the excellent liver to lesion contrast when compared to extracellular contrast agent (33,34). In the present study, 'pseudo

washout' sign is also observed in some cases. This false appearance may lead to the misdiagnosis of HCC. In order to avoid misdiagnosis, only hypo-intensity in the portal venous phase was considered as a 'washout'.

There are several limitations in the present study. Firstly, as the study was performed retrospectively, there may have been selection bias in the study population. In addition, the study sample was relatively small, which may lead to statistical error. Secondly, the histological proof for HCC diagnosis was not obtained for the entire study population, particularly for benign nodules, including hemangioma and adenoma, which were diagnosed by clinical observation and imaging features (35). Clinical diagnostic references, including tumor recurrence following treatment, may not be adequate for HCC diagnosis. Therefore, a prospective study with a large sample size and histologic proof for all nodules should be performed in the future. In addition, the imaging features of nodules with different diameters were not evaluated. Further studies may focus on this issue. Finally, receiver operating characteristic curves were not used to evaluate the diagnostic performance of Gd-EOB-DTPA-enhanced MRI for LI-RADS 4 category nodules, as this method is often used for continuous variables (36).

In conclusion, Gd-EOB-DTPA-enhanced MRI is useful for the diagnosis of HCC LI-RADS 4 category nodules. However, the diagnostic performance of Gd-EOB-DTPA-enhanced MRI for LI-RADS 4 category nodules of different diameters is variable. For hypervascular LI-RADS 4 category nodules with diameter >20 mm, Gd-EOB-DTPA-enhanced MRI is useful for the diagnosis of HCC. However, for hypovascular LI-RADS 4 category nodules with diameter <20 mm, Gd-EOB-DTPA-enhanced MRI may be of limited use due to low diagnostic performance and high FPR.

Acknowledgements

Not applicable.

Funding

No funding was received.

Availability of data and materials

The datasets used and/or analyzed during the current study are available from the corresponding author on reasonable request.

Authors' contributions

QT and CM analyzed and interpreted the patient data. CM was a major contributor in writing the manuscript, and agreed to be accountable for all aspects of the work ensuring that questions related to the accuracy or integrity of any part of the work are appropriately investigated and resolved. All authors read and approved the final manuscript.

Ethics approval and consent to participate

This retrospective study was approved by the Institutional Review Board in accordance with the approved guidelines from The Second XiangYa Hospital of Central South University (Hunan, China) and was compliant with Health Insurance Portability and Accountability Act (HIPAA).

Consent for publication

Written informed consent was obtained from all patients.

Competing interests

The authors declare that they have no competing interests.

References

1. Purysko AS, Remer EM, Coppa CP, Leao HM, Thupili CR and Veniero JC: LI-RADS: A case-based review of the new categorization of liver findings in patients with end-stage liver disease. Radiographics 32: 1977-1995, 2012.
2. Wallace MC, Preen D, Jeffrey GP and Adams LA: The evolving epidemiology of hepatocellular carcinoma: A global perspective. Expert Rev Gastroenterol Hepatol 9: 765-779, 2015.
3. Yan M, Ha J, Aguilar M, Bhuket T, Liu B, Gish RG, Cheung R and Wong RJ: Birth cohort-specific disparities in hepatocellular carcinoma stage at diagnosis, treatment, and long-term survival. J Hepatol 64: 326-332, 2016.
4. Goldberg DS, Valderrama A, Kamalakar R, Sansgiry SS, Babajanyan S and Lewis JD: Hepatocellular carcinoma surveillance among cirrhotic patients with commercial health insurance. J Clin Gastroenterol 50: 258-265, 2016.
5. Bruix J and Sherman M: Management of hepatocellular carcinoma: An update. Hepatology 53: 1020-1022, 2011.
6. Davenport MS, Khalatbari S, Liu PS, Maturen KE, Kaza RK, Wasnik AP, Al-Hawary MM, Glazer DI, Stein EB, Patel J, *et al*: Repeatability of diagnostic features and scoring systems for hepatocellular carcinoma by using MR imaging. Radiology 272: 132-142, 2014.
7. Leoni S, Piscaglia F, Golfieri R, Camaggi V, Vidili G, Pini P and Bolondi L: The impact of vascular and nonvascular findings on the noninvasive diagnosis of small hepatocellular carcinoma based on the EASL and AASLD criteria. Am J Gastroenterol 105: 599-609, 2010.
8. Khalili K, Kim TK, Jang HJ, Haider MA, Khan L, Guindi M and Sherman M: Optimization of imaging diagnosis of 1-2 cm hepatocellular carcinoma: An analysis of diagnostic performance and resource utilization. J Hepatol 54: 723-728, 2011.
9. Santillan C, Chernyak V and Sirlin C: LI-RADS categories: Concepts, definitions, and criteria. Abdom Radiol (NY) 43: 101-110, 2018.
10. Santillan C, Fowler K, Kono Y and Chernyak V: LI-RADS major features: CT, MRI with extracellular agents, and MRI with hepatobiliary agents. Abdom Radiol (NY) 43: 75-81, 2018.
11. Cha DI, Jang KM, Kim SH, Kang TW and Song KD: Liver imaging reporting and data system on CT and gadoxetic acid-enhanced MRI with diffusion-weighted imaging. Eur Radiol 27: 4394-4405, 2017.
12. Granata V, Fusco R, Avallone A, Catalano O, Filice F, Leongito M, Palaia R, Izzo F and Petrillo A: Major and ancillary magnetic resonance features of LI-RADS to assess HCC: An overview and update. Infect Agent Cancer 12: 23, 2017.
13. Chen NX, Motosugi U, Morisaka H, Ichikawa S, Sano K, Ichikawa T Matsuda M, Fujii H and Onishi H: Added value of a gadoxetic acid-enhanced hepatocyte-phase image to the LI-RADS system for diagnosing hepatocellular carcinoma. Magn Reson Med Sci 15: 49-59, 2016.
14. Abd Alkhalik Basha M, Abd El Aziz El Sammak D and El Sammak AA: Diagnostic efficacy of the liver imaging-reporting and data system (LI-RADS) with CT imaging in categorising small nodules (10-20 mm) detected in the cirrhotic liver at screening ultrasound. Clin Radiol 72: 901.e1-901.e11, 2017.
15. Mitchell DG, Bruix J, Sherman M and Sirlin CB: LI-RADS (Liver Imaging Reporting and Data System): Summary, discussion, and consensus of the LI-RADS management working group and future directions. Hepatology 61: 1056-1065, 2015.
16. Santillan CS, Tang A, Cruite I, Shah A and Sirlin CB: Understanding LI-RADS: A primer for practical use. Magn Reson Imaging Clin N Am 22: 337-352, 2014.

17. Elsayes KM, Hooker JC, Agrons MM, Kielar AZ, Tang A, Fowler KJ, Chernyak V, Bashir MR, Kono Y, Do RK, *et al*: 2017 Version of LI-RADS for CT and MR Imaging: An Update. Radiographics 37: 1994-2017, 2017.
18. Qian H, Li S, Ji M and Lin G: MRI characteristics for the differential diagnosis of benign and malignant small solitary hypovascular hepatic nodules. Eur J Gastroen Hepat 28: 749-756, 2016.
19. Joo I, Lee JM, Lee SM, Lee JS, Park JY and Han JK: Diagnostic accuracy of liver imaging reporting and data system (LI-RADS) v2014 for intrahepatic mass-forming cholangiocarcinomas in patients with chronic liver disease on gadoxetic acid-enhanced MRI. J Magn Reson Imaging 76: 1330-1338, 2016.
20. Motosugi U, Ichikawa T, Onohara K, Sou H, Sano K, Muhi A and Araki T: Distinguishing hepatic metastasis from hemangioma using gadoxetic acid-enhanced magnetic resonance imaging. Invest Radiol 46: 359-365, 2011.
21. Darnell A, Forner A, Rimola J, Reig M, Garcia-Criado A, Ayuso C and Bruix J: Liver imaging reporting and data system with MR imaging: Evaluation in nodules 20 mm or smaller detected in cirrhosis at screening US. Radiology 275: 698-707, 2015.
22. Di Pietropaolo M, Briani C, Federici GF, Marignani M, Begini P, Delle Fave G and Iannicelli E: Comparison of diffusion-weighted imaging and gadoxetic acid-enhanced MR images in the evaluation of hepatocellular carcinoma and hypovascular hepatocellular nodules. Clin Imag 39: 468-475, 2015.
23. Motosugi U, Bannas P, Sano K and Reeder SB: Hepatobiliary MR contrast agents in hypovascular hepatocellular carcinoma. J Magn Reson Imaging 41: 251-265, 2015.
24. Ichikawa S, Ichikawa T, Motosugi U, Sano K, Morisaka H, Enomoto N, Matsuda M, Fujii H and Araki T: Presence of a hypovascular hepatic nodule showing hypointensity on hepatocyte-phase image is a risk factor for hypervascular hepatocellular carcinoma. J Magn Reson Imaging 39: 293-297, 2014.
25. Golfieri R, Renzulli M, Lucidi V, Corcioni B, Trevisani F and Bolondi L: Contribution of the hepatobiliary phase of Gd-EOB-DTPA-enhanced MRI to dynamic MRI in the detection of hypovascular small (<=2 cm) HCC in cirrhosis. Eur Radiol 21: 1233-1242, 2011.
26. Quaia E, De Paoli L, Pizzolato R, Angileri R, Pantano E, Degrassi F, Ukmar M and Cova MA: Predictors of dysplastic nodule diagnosis in patients with liver cirrhosis on unenhanced and gadobenate dimeglumine-enhanced MRI with dynamic and hepatobiliary phase. AJR Am J Roentgenol 200: 553-562, 2013.
27. Kang Y, Lee JM, Kim SH, Han JK and Choi BI: Intrahepatic mass-forming cholangiocarcinoma: Enhancement patterns on gadoxetic acid-enhanced MR images. Radiology 264: 751-760, 2012.
28. Xu J, Igarashi S, Sasaki M, Matsubara T, Yoneda N, Kozaka K, Ikeda H, Kim J, Yu E, Matsui O, *et al*: Intrahepatic cholangiocarcinomas in cirrhosis are hypervascular in comparison with those in normal livers. Liver Int 32: 1156-1164, 2012.
29. Rimola J, Forner A, Reig M, Vilana R, de Lope CR, Ayuso C and Bruix J: Cholangiocarcinoma in cirrhosis: Absence of contrast washout in delayed phases by magnetic resonance imaging avoids misdiagnosis of hepatocellular carcinoma. Hepatology 50: 791-798, 2009.
30. Joo I, Lee JM, Lee DH, Jeon JH, Han JK and Choi BI: Noninvasive diagnosis of hepatocellular carcinoma on gadoxetic acid-enhanced MRI: Can hypointensity on the hepatobiliary phase be used as an alternative to washout? Eur Radiol 25: 2859-2868, 2015.
31. Loyer EM, Chin H, DuBrow RA, David CL, Eftekhari F and Charnsangavej C: Hepatocellular carcinoma and intrahepatic peripheral cholangiocarcinoma: Enhancement patterns with quadruple phase helical CT-a comparative study. Radiology 212: 866-875, 1999.
32. Goshima S, Kanematsu M, Kondo H, Yokoyama R, Kajita K, Tsuge Y, Shiratori Y, Onozuka M and Moriyama N: Hepatic hemangioma: Correlation of enhancement types with diffusion-weighted MR findings and apparent diffusion coefficients. Eur J Radiol 70: 325-330, 2009.
33. Tateyama A, Fukukura Y, Takumi K, Shindo T, Kumagae Y and Nakamura F: Hepatic hemangiomas: factors associated with pseudo washout sign on Gd-EOB-DTPA-enhanced MR imaging. Magn Reson Med Sci 15: 73-82, 2016.
34. Kim B, Byun JH, Kim HJ, Won HJ, Kim SY, Shin YM and Kim PN: Enhancement patterns and pseudo-washout of hepatic haemangiomas on gadoxetate disodium-enhanced liver MRI. Eur Radiol 26: 191-198, 2016.
35. Grazioli L, Ambrosini R, Frittoli B, Grazioli M and Morone M: Primary benign liver lesions. Eur J Radiol 95: 378-398, 2017.
36. Kumar R and Indrayan A: Receiver operating characteristic (ROC) curve for medical researchers. Indian Pediatr 48: 277-287, 2011.